

Modelling of Phase Boundaries via the GAUSS-Point Method

J. Kreikemeier

In this paper an evaluation of the GAUSS-point method to describe material boundaries is presented. This numerically based method uses the geometrical location of the integration points of the finite elements to decide for one material or another. In contrast to well established alternative approaches like, e.g., the conforming mesh method, the GAUSS-point method allows to use a fully structured finite element mesh. It is shown in this contribution that the number of integration points used to describe the corresponding constitutive phase is the fundamental parameter to control and to adjust the stiffness properties onto the real values. Numerical predictions of the effective material properties of a single fibre embedded within a matrix material are carried out for three different finite element mesh densities and are compared to the reference of the conforming mesh method.

1 Introduction

Fibre reinforced composites are usually made from longitudinally aligned fibres within a matrix material. The mechanical properties of all of the constituents differ from each other, e.g., the YOUNG's modulus of a single glass fibre is orders of magnitudes larger compared to a standard resin material and the fracture strain of the matrix material should be twice as large as the fracture strain of the fibres to fully exploit the fibre strength capabilities, Altenbach et al. (1996). Thus phase boundaries emerge between one material and another and the constitutive description of heterogeneous materials is a challenging task. The mathematical description of phase boundaries can be treated principally by two different approaches. The first one assumes that the separation of the boundaries at the interphases during deformation is allowed. Hence phenomena like, e.g., crack opening and crack propagation can be observed. The mathematical description is normally based on linear elastic fracture mechanics assumptions or cohesive zone approaches. The second method assumes a perfect bonding between the material phases, thus there is no separation of the several materials allowed. If one is interested in the constitutive description of a multi phase material alone, the second approach is sufficient. So it is done in this paper.

For finite element based modelling approaches the use of a phase boundary conforming finite element mesh is the most accurate possibility to take into account the heterogeneities within a material. Each finite element consists of just one material and there is no discontinuity within the stiffness components of the element. In the work of Löhnert (2004) the method of hanging nodes is introduced to account for phase boundaries. This method is based on a mesh refinement in regions of phase boundaries. The degrees of freedom of these hanging nodes therefore depend on the degrees of freedom of the element the hanging nodes are connected to. The definition of an implicit level set curve to track moving interfaces was done by Osher and Sethian (1988). The phase boundary is represented by an implicit level set curve of a higher order function. The big advantage of this method is the possibility of an interface independent finite element meshing, see, e.g. Sukumar et al. (2001) for an interface modelling within the framework of extended finite element method. In this presentation the level set functions are used as enrichment functions for the additional degrees of freedom. In Figure 1 the hanging node method as well as the level set method are principally shown.

Beside the interface modelling strategies mentioned above, the GAUSS-point method enables the observance of interfaces or phase boundaries by the use of structured and undistorted finite element meshes, Figure 2. Therefore the meshing effort is very low but a single finite element may appear more complex, because the definition of more than one material within it is possible, which leads to discontinuities within the stiffness values, Zohdi et al. (1998). First of all in Steinkopff (1995) the use of multiphase finite elements was proposed to account for a simple finite element mesh for the adaption of the microstructural geometry of Ag-Ni composites. It was pointed out that the exact position of phase boundaries is lost, which may cause an artificial change of constituent volume fraction. To overcome this the use of very fine finite element meshes was propounded. In conclusion the obtained numerical results were in a good agreement with respect to the rezoning algorithm model at much less effort for model generation and minimum cpu time. In Lippmann et al. (1996a) the use of multiphase finite elements to study the failure mechanisms in AlSi cast alloys with varying microstructures is presented. Therefore experimental in-situ

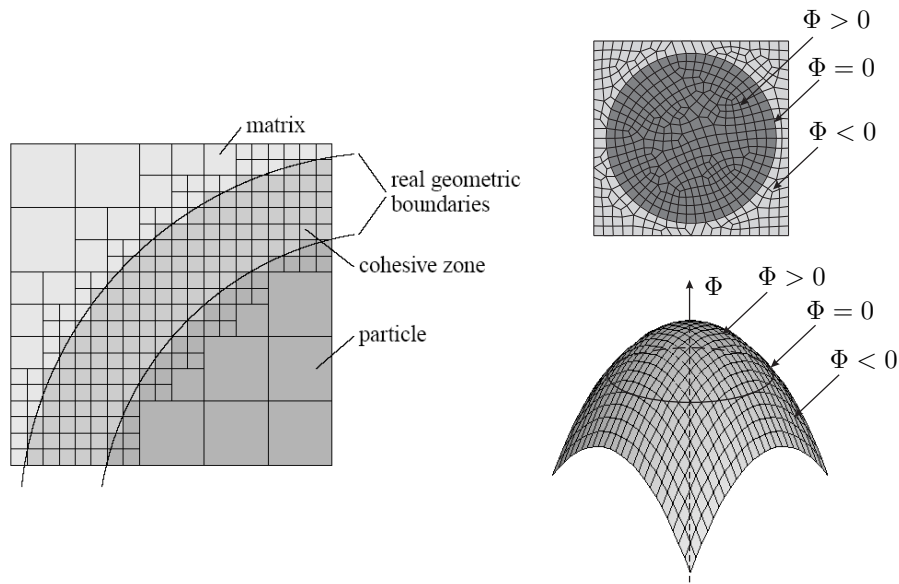


Figure 1: The hanging node method, Löhnert (2004), as well as the level set method, Osher and Sethian (1988), to build up phase boundaries (from left).

tensile tests in conjunction with scanning electron microscopy were carried out a priori. The method of multiphase elements is used to embed representative microstructural cells into a 2D model of the in-situ tensile test specimens. The results therefore were in qualitatively good agreement with the experiments. An exploitation to 3D multiphase finite elements is given in Lippmann et al. (1996b) to simulate both a single fibre within a matrix material as well as complex microstructures, respectively. The morphology of real constituents is introduced into the finite element model via digitized images of the microstructure which are superimposed on the finite element mesh. By the geometrical location of the integration points the assignment of the different materials is carried out. This was the first 3D implementation of the multiphase finite elements in a commercial finite element code. In Wulf et al. (1996) ductile failure of Al(6061)/SiC composites is simulated by means of multiphase elements in conjunction with automatic element elimination technique.

In conclusion the application of multiphase finite element method, which is called the GAUSS-point in this work, is a promising modelling alternative to the conforming mesh method or the hanging node method, respectively.

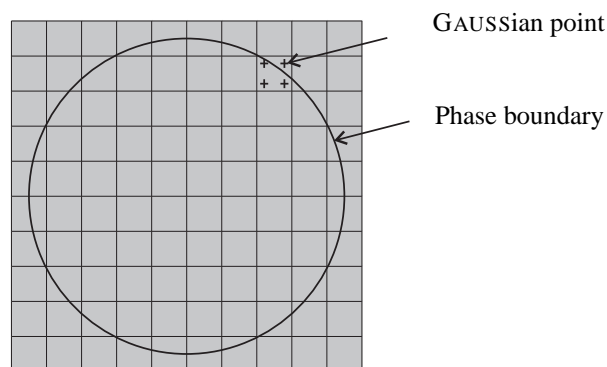


Figure 2: The GAUSS-point method to define internal boundaries. By means of the geometrical location each GAUSSian point can be assigned to one constitutive phase or another. The GAUSSian points within the inner of the circle belong to one phase, whereas the rest of the GAUSSian points affiliate to the second phase, respectively.

Notation:

Throughout the text a direct tensor notation is preferred. If necessary an index notation using the summation convention will be used to avoid the definition of new symbols. Vectors are denoted by lowercase bold letters $\mathbf{a} = a_i \mathbf{e}_i$ where \mathbf{e}_i denote the orthonormal base vectors. A second order tensor is represented by an uppercase bold letter $\mathbf{A} = A_{ij} \mathbf{e}_i \otimes \mathbf{e}_j$. Tensors of fourth order are symbolised like \mathbf{C} . A dot represents one scalar contraction,

e.g., $\mathbf{a} = \mathbf{A} \cdot \mathbf{b}$ and $\mathbf{A} = \mathbb{C} \cdot \mathbf{B}$.

2 Evaluation of the GAUSS-Point Method

2.1 The Representative Volume Element Technology

The evaluation of the GAUSS-point method with respect to the conforming mesh method will be given for the calculation of effective properties of a representative volume element (RVE). The RVE consists of a single fibre which is embedded into a matrix material. The RVE technique is a methodology to obtain effective material properties both analytically and/or numerically. The foundations of RVE modelling especially regarding the minimum size which is necessary for the RVE to be representative can be found in Bishop and Hill (1951a), Bishop and Hill (1951b) or Hill (1952). Originally focused on the description of polycrystalline aggregates the RVE is of sufficient size, if it contains a sufficiently large number of grains and if it is macroscopically homogeneous, Bishop and Hill (1951a) and Bishop and Hill (1951b).

It is important to define the size of the RVE to be small enough compared to the macroscopic material point and to be large enough to contain a sufficient number of different phases or constituents to be representative. Therefore a possible criterion is the HILL condition which states the equivalence of the stress power calculated by means of the micro information and by the macro information. In linear theory the volume average of the infinitesimal strain tensor is equal to the infinitesimal strain tensor at the boundary of the RVE. When using nonlinear strain measures, e.g., the GREEN strain tensor $\bar{\mathbf{E}}$, the stress and strain measures for homogenisation must be linear dependent on the displacement to fulfill the HILL condition. Thus the deformation gradient $\bar{\mathbf{F}}$ in conjunction with the work conjugated first PIOLA-KIRCHHOFF stress tensor $\bar{\mathbf{T}}^{1PK}$ are often used for the homogenisation procedure, Böhlke (2001) and Kreikemeier (2011).

One important requirement on the RVE is the periodicity of the boundary surfaces, i.e., overlapping or gapping of boundary surfaces must be prevented. In order to do so, a displacement of the form

$$\mathbf{u}(\mathbf{X}, t) = \bar{\mathbf{H}}(t) \cdot \mathbf{X} + \mathbf{w}(\mathbf{X}, t) \quad (1)$$

is defined, where $\bar{\mathbf{H}}(t)$ denotes the mean displacement gradient, \mathbf{X} is the material position vector and $\mathbf{w}(\mathbf{X}, t)$ is the local fluctuation vector, respectively. In the case of homogeneous displacement boundary conditions spatially constant or linear fields of displacement are prescribed on all boundaries of the RVE. In the case of a homogeneous material this results in a deformation of the RVE which would be constant in space or homogeneous $\mathbf{w}(\mathbf{X}, t) = \mathbf{0}$, Bertram (2008). The most accurate results are normally achieved by applying periodic boundary conditions, so it is done here. The nodal displacements \mathbf{u}^A and \mathbf{u}^B on opposing surface points A and B of the RVE should be

$$\mathbf{u}^A = \bar{\mathbf{H}} \cdot \mathbf{X}^A + \mathbf{w}(\mathbf{X}^A) \quad \text{and} \quad (2)$$

$$\mathbf{u}^B = \bar{\mathbf{H}} \cdot \mathbf{X}^B + \mathbf{w}(\mathbf{X}^B). \quad (3)$$

It is now assumed that $\mathbf{w}(\mathbf{X}^A) = \mathbf{w}(\mathbf{X}^B)$ must hold for periodicity reasons, thus

$$\mathbf{u}^B = \mathbf{u}^A + \bar{\mathbf{H}} \cdot (\mathbf{X}^B - \mathbf{X}^A) = \mathbf{u}^A + \bar{\mathbf{H}} \cdot \Delta \mathbf{X}. \quad (4)$$

Furthermore the equilibrium of the stress vector field on opposite boundaries of the RVE is assumed, too

$$\mathbf{t}^A(\mathbf{X}, t) = -\mathbf{t}^B(\mathbf{X}, t). \quad (5)$$

A sketch of periodic boundary conditions is shown in Figure 3.

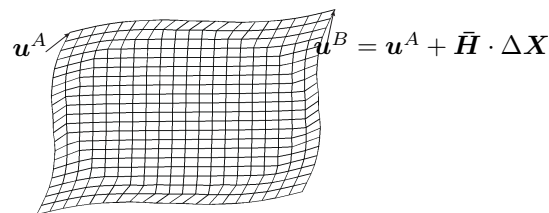


Figure 3: Definition of periodic boundary conditions to ensure the periodicity of the RVE, Kreikemeier (2011).

2.2 Numerical Model Adaption

As pointed out above the evaluation of the GAUSS-point method with respect to the conforming mesh method is carried out on a single fibre RVE with a square fibre arrangement. The intention is to estimate the corresponding effective stiffness values for different fibre volume fractions and different mesh sizes, respectively. The fibre volume fractions range from $\varphi = 0.1$ to $\varphi = 0.7$ with an incrementation of $\Delta\varphi = 0.1$. The fibre is made from isotropic glass with

$$E_f = 70000 \text{ MPa}, \quad (6)$$

$$\nu_f = 0.4. \quad (7)$$

As matrix material an isotropic and unsaturated polyester resin is assumed with

$$E_m = 3500 \text{ MPa}, \quad (8)$$

$$\nu_m = 0.3. \quad (9)$$

On the surfaces of the RVE's periodic displacement boundary conditions are defined to ensure no overlapping or gapping on neighboring RVE surfaces. When using long glass fibre reinforced plastic materials the effective material behaviour exhibits transverse isotropy, i.e., there are five independent material parameters necessary to describe the constitutive relation within a closed manner. The effective constitutive relation is then given by

$$\bar{\mathbf{T}} = \bar{\mathbf{C}} \cdot \bar{\mathbf{E}}, \quad (10)$$

where $\bar{\mathbf{T}}$ denotes the effective second PIOLA-KIRCHHOFF stress tensor. This relation can be simplified, if vector matrix notation is used

$$\begin{bmatrix} \bar{T}_{11} \\ \bar{T}_{22} \\ \bar{T}_{33} \\ \bar{T}_{12} \\ \bar{T}_{13} \\ \bar{T}_{23} \end{bmatrix} = \begin{bmatrix} \bar{C}_{1111} & \bar{C}_{1122} & \bar{C}_{1122} & 0 & 0 & 0 \\ & \bar{C}_{2222} & \bar{C}_{2233} & 0 & 0 & 0 \\ & & \bar{C}_{2222} & 0 & 0 & 0 \\ & & & \bar{C}_{1212} & 0 & 0 \\ & & & & \bar{C}_{1212} & 0 \\ & & & & & \frac{1}{2}(\bar{C}_{2222} - \bar{C}_{2233}) \end{bmatrix} \begin{bmatrix} \bar{E}_{11} \\ \bar{E}_{22} \\ \bar{E}_{33} \\ \bar{E}_{12} \\ \bar{E}_{13} \\ \bar{E}_{23} \end{bmatrix}. \quad (11)$$

It is pointed out here, that the use of a normalisation of the basis dyads is always recommended to ensure an orthonormal basis system. Due to use of vector matrix notation just to represent the effective material parameters a normalisation is omitted here. In order to identify the characteristics of the GAUSS-point method three different mesh densities with $1 \times 10 \times 10$, $1 \times 20 \times 20$ as well as $1 \times 30 \times 30$ finite elements of the RVE are investigated, respectively. The longitudinal fibre direction is assumed to be the 1-axis.

The assessment of the effective material properties obtained is carried out by means of the relative error

$$\Delta^{rel} = \frac{\bar{C}_{ijkl}^{GP} - \bar{C}_{ijkl}^{CM}}{\bar{C}_{ijkl}^{CM}}, \quad (12)$$

where \bar{C}_{ijkl}^{GP} denote the effective material properties obtained by the GAUSS-point method and \bar{C}_{ijkl}^{CM} are the effective properties estimated by the conforming mesh method, respectively.

The finite element meshes of the GAUSS-point method and of the conforming mesh method for a fibre volume fraction of $\varphi = 0.10$ and $\varphi = 0.70$ are shown in Figures 4 and 5. As can be seen the finer the mesh of the RVE defined by the GAUSS-point method the more GAUSSian points are used to build up the distinct constitutive phases. A problem regarding the GAUSS-point method must be seen within the too stiff constitutive response on outer loading especially in the transverse fibre directions, which makes the use of this method always a challenging task, Zohdi et al. (1998).

We will see below the regimes of validity with respect to the mesh sizes compared to the conforming mesh method.

2.2.1 Comparison of the Effective Properties

In the following Figures the effective material properties obtained by the conforming mesh method and by the GAUSS-point method as well as the corresponding relative errors are shown. The stiffness values on the left hand

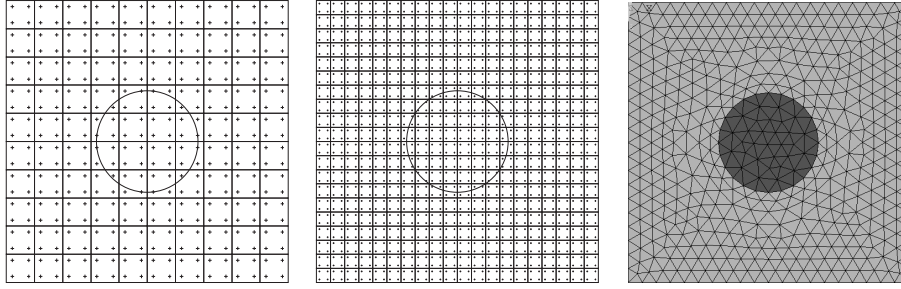


Figure 4: Two GAUSS-point meshes and the conforming mesh for $\varphi = 0.10$.

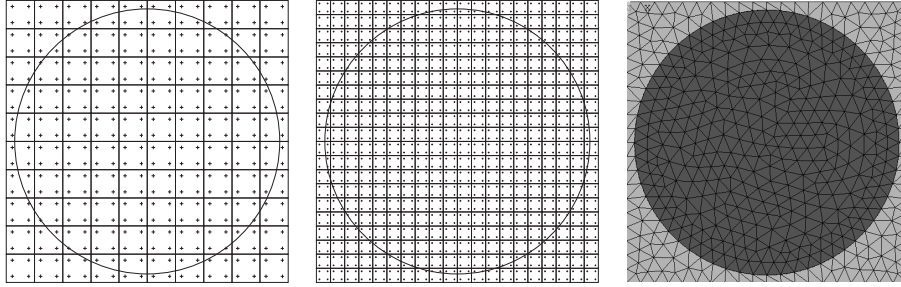


Figure 5: Two GAUSS-point meshes and the conforming mesh for $\varphi = 0.70$.

side of the Figures are given in [MPa]. As can be seen there is an excellent agreement of the effective stiffness values \bar{C}_{1111} in fibre direction with respect to the conforming mesh method for a mesh size of $1 \times 30 \times 30$ elements for all fibre volume fractions, Figure 6. The relative error is always $\Delta^{rel} < 0.03$. In the case of $1 \times 20 \times 20$ mesh size the corresponding relative error is $\Delta^{rel} < 0.03$, too. Only for a fibre volume fraction of $\varphi = 0.70$ there is a notable deviation and the relative error raises to $\Delta^{rel} > 0.15$. As expected the mesh size of $1 \times 10 \times 10$ delivers the most sensitive results. Up to a fibre volume fraction of $\varphi < 0.52$ the predictions are within an excellent agreement. Thereafter however the relative error raises to $\Delta^{rel} \approx 0.30$.

In contrast to the effective longitudinal stiffness value prediction the predictions of the effective transverse stiffness values \bar{C}_{2222} and \bar{C}_{3333} as well as the effective shearing components \bar{C}_{1122} , \bar{C}_{1133} , \bar{C}_{2233} and the components \bar{C}_{1212} and \bar{C}_{1313} show large discrepancies for the RVE with $1 \times 10 \times 10$ meshing and fibre volume fractions of $\varphi = 0.21$ and $\varphi = 0.41$, 7 to 10. The fibre geometry approximation in these cases is a rather rough one, i.e., the geometry is not of circular cross section but appears more cross like, Figure 11, which obviously strongly influences the transverse material properties. Thus the geometry approximation is not that smooth and the constitutive response is too stiff in transverse fibre direction and in shearing, respectively.

To overcome this phenomenon a finer mesh to define the RVE can be used. One notices a slight overestimation within all transverse effective stiffness values for a mesh size of $1 \times 20 \times 20$ elements up to $\varphi = 0.6$. If $\varphi > 0.6$ the effective stiffness value prediction differs from the effective values obtained by the conforming mesh method. As expected the $1 \times 30 \times 30$ meshing delivers the best effective property predictions for the transverse stiffness values as well as for the shearing components, again. The relative errors therefore are all $\Delta^{rel} < 0.03$. This meshing seems to be the minimum discretisation which is necessary to predict effective stiffness values for a single fibre RVE within a sufficient manner for all fibre volume fractions.

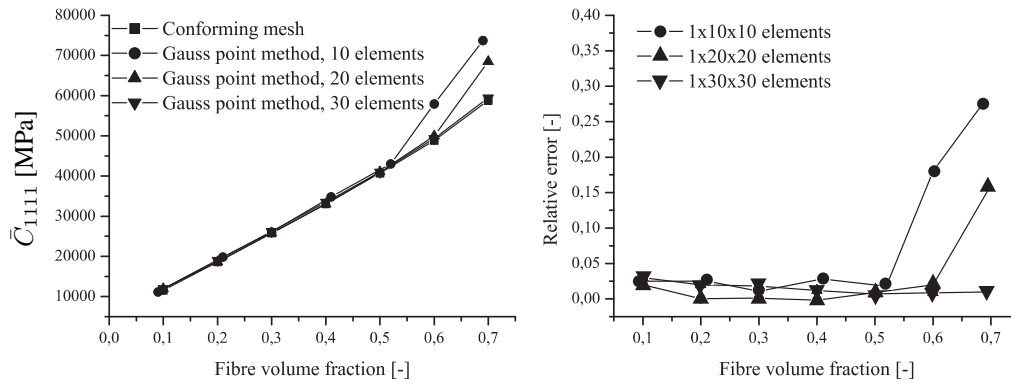


Figure 6: Comparison of \bar{C}_{1111} values predicted by GAUSS-point method and conforming mesh method, respectively.

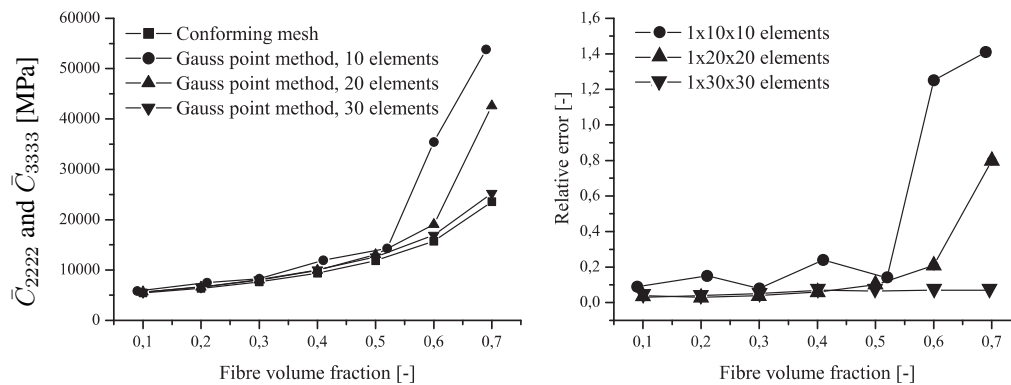


Figure 7: \bar{C}_{2222} and \bar{C}_{3333} values predicted by GAUSS-point method and conforming mesh method, respectively.

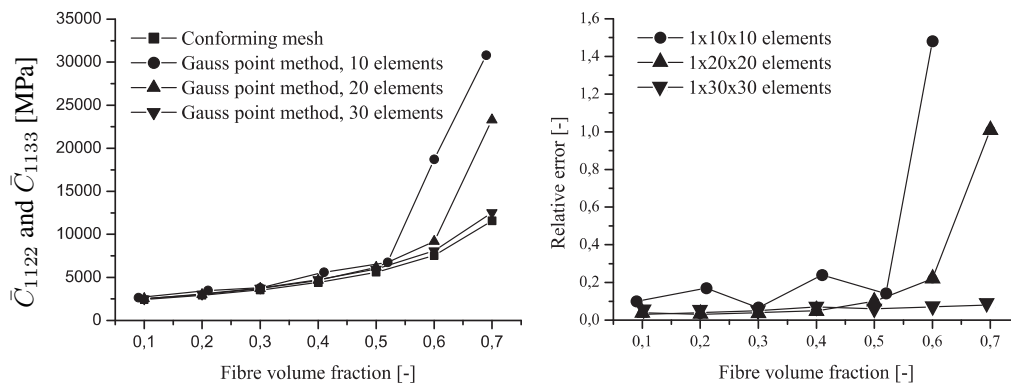


Figure 8: \bar{C}_{1122} and \bar{C}_{1133} values predicted by GAUSS-point method and conforming mesh method, respectively.

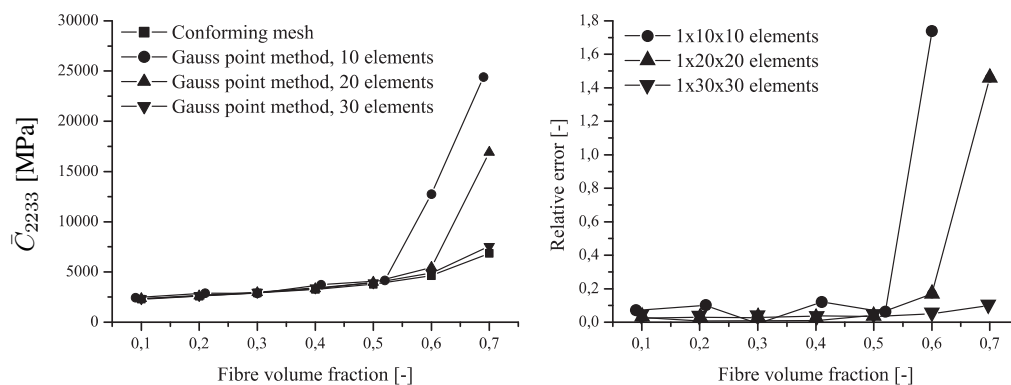


Figure 9: \bar{C}_{2233} values predicted by GAUSS-point method and conforming mesh method, respectively.

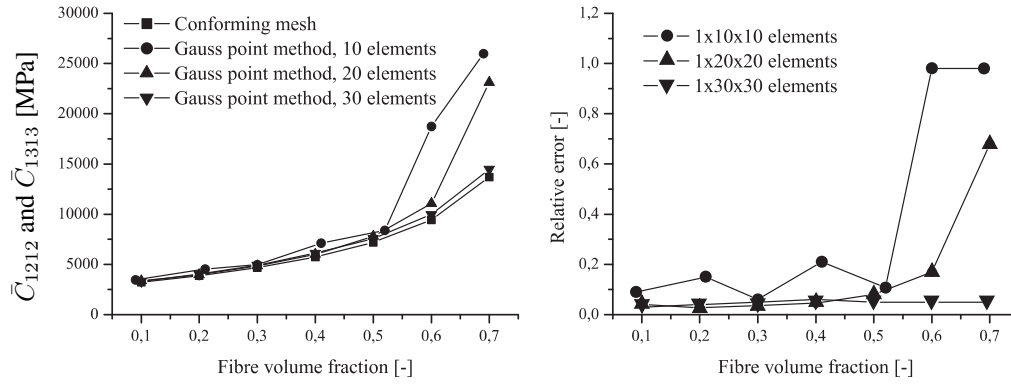


Figure 10: \bar{C}_{1212} and \bar{C}_{1313} values predicted by GAUSS-point method and conforming mesh method, respectively.

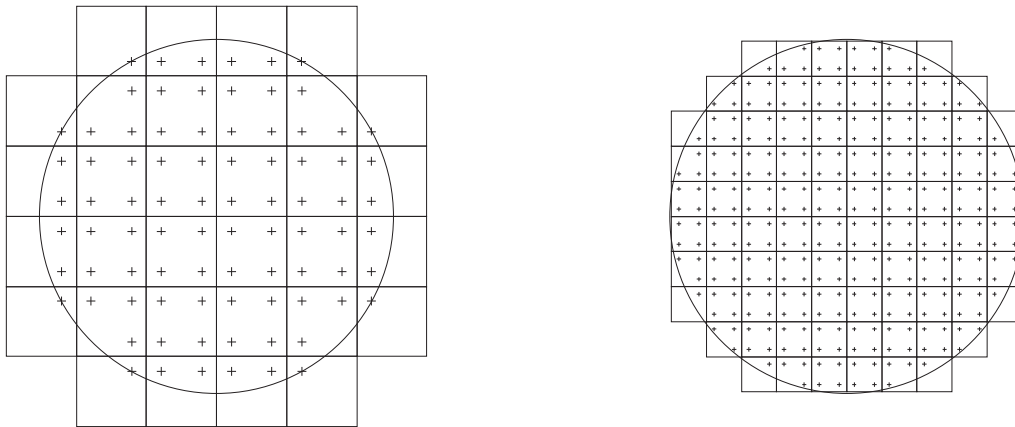


Figure 11: Fibre geometry approximation by different mesh sizes for $\varphi = 0.21$.

When using the $1 \times 10 \times 10$ discretisation the fibre geometry strongly differs from the circular geometry (left). If $1 \times 20 \times 20$ elements are used to discretise the RVE the fibre geometry approximation narrows the real circular fibre geometry in a more sufficient way.

3 Conclusion and Outlook

In this paper an evaluation of the GAUSS-point method to describe phase boundaries was given. Indeed this method is usually of less quality compared to the conforming mesh method or other approaches, it can be advantageous to apply.

For the evaluation of this method a representative volume element (RVE) was used to estimate the effective material properties of a single glass fibre embedded within a matrix material for different fibre volume fractions as well as different finite element mesh densities. The predictions of the effective material properties in fibre direction were satisfying for all mesh sizes up to a fibre volume fraction of $\varphi = 0.52$. In contrast to this a strong dependence on the mesh size was revealed for the effective properties in the transverse fibre directions. Here the coarse meshes of $1 \times 10 \times 10$ and $1 \times 20 \times 20$ delivered very stiff predictions compared to the conforming mesh method. Just the results obtained by the $1 \times 30 \times 30$ RVE showed a very good agreement with respect to the conforming mesh approach in the transverse fibre directions, too. The relative errors were less than 0.03. One concludes that the $1 \times 30 \times 30$ meshing seems to be the minimum discretisation to predict the effective material properties of a single fibre RVE for all fibre volume fractions within a sufficient manner.

Further work focuses on the investigation of the GAUSS-point method in the case of more complex micro structures, e.g., particle reinforced composites or short fibre reinforced composites in connection with multi scale modelling strategies for the constitutive modelling.

References

- Altenbach, H.; Altenbach, J.; Rikard, R.: *Einführung in die Mechanik der Laminat- und Sandwichtragwerke*. Deutscher Verlag für Grundstoffindustrie Stuttgart (1996).
- Bertram, A.: *Elasticity and Plasticity of Large Deformations*. Springer (2008).
- Bishop, J.; Hill, R.: A theoretical derivation of the plastic properties of a polycrystalline face-centred material. *Phil. Mag.*, 42, (1951a), 1298–1307.
- Bishop, J.; Hill, R.: A theory of plastic distortion of a polycrystalline aggregate. *Phil. Mag.*, 42, (1951b), 414–427.
- Böhlke, T.: *Crystallographic Texture Evolution and Elastic Anisotropy - Simulation Modeling and Applications*. Shaker-Verlag (2001).
- Hill, R.: The elastic behaviour of a crystalline aggregate. *Proc.R.Soc.Lond.A*, 65, (1952), 349–354.
- Kreikemeier, J.: *A Two Scale Finite - Element - Approach to Analyse the Damage State of Composite Structures*. Forschungsbericht 2011-5, Deutsches Zentrum für Luft- und Raumfahrt e.V. in der Helmholtz-Gemeinschaft (2011).
- Lippmann, N.; Schmauder, P.; Gumbsch, P.: Numerical and Experimental Study of the Failure Mechanisms in AlSi-Cast Alloys. In: H. Nisitani; M. Aliabadi; S. Isida; D. Cartwright, eds., *Localised Damage 96*, Computer Aided Assessment and Control 3-5 June 1996, Fukuoka, Japan, 333–340, Computational Mechanics Publications (1996a).
- Lippmann, N.; Steinkopff, T.; Schmauder, P.; Gumbsch, P.: 3D-Finite-Element-Modelling of Microstructures with the Method of Multiphase elements. In: M. Rappaz; M. Kedro, eds., *Conference Proceedings Modelling in Materials Science and Process*, 404–410, ECSC-EC-EACE Brussels, Belgium, 1996 (1996b).
- Löhnert, S.: *Computational Homogenization of Microheterogeneous Materials at Finite Strains Including Damage*. Universität Hannover (2004).
- Osher, S.; Sethian, J.: Fronts propagating with curvature- dependent speed: Algorithms based on hamilton-jacobi formulations. *J.Comput.Phys.*, 79, (1988), 12–49.
- Steinkopff, M., Th. nad Sautter: Simulating the elasto-plastic behaviour of multiphase materials by advanced finite element techniques. *Comp.Mat.Sci.*, 4, (1995), 10–14;15–22.
- Sukumar, N.; Chopp, D.; Moes, N.; Belytschko, T.: Modeling holes and inclusions by level sets in the extended finite-element method. *Comput.Methods Appl.Mech.Engng.*, 190, (2001), 6183–6200.

Wulf, J.; Steinkopff, T.; Fischmeister, H.: FE-Simulation of Crack Paths in the Real Microstructure of an Al(6061)/SiC Composite. *Acta Materialia*, 44(5), (1996), 1765–1779.

Zohdi, T.; Feucht, M.; Gross, D.; Wriggers, P.: A description of macroscopic damage through microstructural relaxation. *Int.J.Numer.Meth.Engng.*, 43, (1998), 493–506.

Address: Dr.-Ing. Janko Kreikemeier, Deutsches Zentrum für Luft- und Raumfahrt e.V., Institut für Faserverbundleichtbau und Adaptronik, Strukturmechanik, D-38108 Braunschweig.
email: janko.kreikemeier@dlr.de.